1

Past loggings, drought and pathogens interact and contribute to forest dieback

4

Gabriel Sangüesa-Barreda[1]*, J. Julio Camarero[1], Jonàs Oliva[2], Fernando Montes[3] and

Antonio Gazol[1]

[1]Instituto Pirenaico de Ecología (CSIC). Avda. Montañana 1005, Apdo. 202, 50192

Zaragoza, Spain.

[2]Department of Forest Mycology and Plant Pathology, Swedish University of

Agricultural Sciences, Box 7026, S-750 07 Uppsala, Sweden

[3]Centre for Forest Research, INIA. Ctra. A Coruña, km 7.5, 28040 Madrid, Spain

12

*Corresponding author:

Gabriel Sangüesa Barreda

Instituto Pirenaico de Ecología, CSIC.

Avenida Montañana 1005, Zaragoza E-50192, Spain.

Phone: (+34) 976-369-393 ext .880040

E-mail: gsanguesa@ipe.csic.es

19

Abstract

Forest dieback is one of the most widespread responses to global-change drivers such as climate warming-related drought stress and the spread of pathogens. Although both climatic and biotic stressors have been studied separately, much less is known on how drought and pathogens interact and induce dieback, particularly in formerly used forests. We determine the roles played by each of those drivers as factors causing recent dieback in three Pyrenean silver fir stands: a managed site subjected to past logging and two unmanaged sites not logged for the past fifty years. The age, size, recent competition, and basal-area increment (BAI) trends of non-declining and declining trees, and the presence of fungal pathogens were investigated. Growth patterns at yearly to decadal time scales were compared to distinguish the roles and interactions played by the different stressors. In the managed site, declining trees displayed low growth already before logging (1950s-1970s). In both unmanaged sites, declining and non-declining trees displayed divergent growth patterns after extreme droughts, indicating that dieback was triggered by severe water deficit. We did not find indications that fungal pathogens are the primary drivers of dieback since a low proportion of declining trees were infested by primary pathogens (10%). However, trees with the primary fungal pathogen *Heterobasidion* showed lower BAI than non-declining trees. On the other hand, the secondary fungal pathogen *Amylostereum* was isolated from a higher number of trees than expected by chance. These findings highlight the importance of legacies such as the past use in driving recent forest dieback. Past forest use could predispose to dieback by selecting slow-growing trees and thus making some them more vulnerable to drought and fungal pathogens.

46   **Highlights**

47   • How droughts, pathogens and past use interact and induce silver fir dieback?
48   • Dieback was triggered by severe droughts.
49   • Trees infected with primary fungal pathogens showed lower growth rates.
50   • In the managed site dieback was related to past use and recent droughts.
51   • Past forest use predisposes to dieback by selecting slow-growing trees.

52

1. Introduction

Global-change drivers such as climate warming and aridification, land-use modifications and biotic agents alter the structure, dynamics, services and functioning of forests (Bonan, 2008). Forest dieback and the consequent massive tree mortality events are becoming prominent responses to those drivers, questioning the ability of many forests to act as carbon sinks (Dobbertin et al., 2007; Allen et al., 2010). Therefore, understanding and modelling the roles and interactions played by these drivers, which act at different temporal and spatial (region, stand and tree) scales, is challenging ecologists who are trying to determine the cause–effect relationships and their relative importance (McDowell et al., 2013).

Climatic stressors such as droughts are probably the best-characterized causes of forest dieback in diverse biomes around the world (see Bigler et al., 2006, 2007; Adams et al., 2009; Van Mantgen et al., 2009; Williams et al., 2013; Cailleret et al., 2014; Zhang et al., 2014). Most authors have treated separately drought-induced and pathogen-driven forest mortality cases but this division is arbitrary since pathogens usually attack trees already stressed by drought (McDowell et al., 2013). Therefore, to understand how dieback proceeds we must consider how all potential dieback factors (drought, biotic agents) interact and if they are related to past forest modifications by humans (such as structure changes or fires). Fungal pathogens are one of the most important drivers in the final phase of drought-induced mortality (Oliva et al., 2014); however, despite its importance, little is known about fungal diseases with regard to quantified information, spatial-temporal effects or their relationship with other stressors. First, it has been postulated that climate warming will increase the impact of pathogens on forests; however, the abundance of those biotic stressors may also depend on changes in the forest structure (e.g., past thinning) (Oliva et al., 2009; Oliva and

Colinas, 2010), which determine recent tree-to-tree competition (Ayres and Lombardero, 2000). For instance, past thinning creates stumps, which act as expansion foci for several root-rot fungi, thus making trees more vulnerable to drought by reducing their vigour and growth (Oliva et al., 2014). Second, in Europe the abandonment of traditional forest use and changing conservation policies have contributed to the increase in tree density and cover, leading to increased competition between trees. Such densification could increase the competition for water between neighbouring trees in mesic sites during dry periods or in drought-prone areas, predisposing trees to dieback (Linares et al., 2010). Third, it is expected that pathogens may interact with drought stress, potentially leading to non-linear (threshold-type) responses in tree vigour and growth, which will require new analytical approaches (Camarero et al., 2014). Fourth, little is known about the involvement of pathogens in long-term dieback processes. For example, Manion (1991) considered fungal pathogens as opportunistic factors affecting previously stressed trees; however, pathogens could also act as primary drivers of dieback (Oliva et al., 2014). Last but not least, one should consider the role played by selective cuttings in changing the structure of the stand. Selective cuttings mainly remove the largest trees, leaving some big trees to produce seeds and smaller trees to provide protection to the incoming regeneration. It has been hypothesized that dieback mainly affects less-vigorous trees that are unable to adapt to the new conditions of the stand that are created as a result of the cuttings (Oliva and Colinas, 2007). To address these issues and to forecast how vulnerable forests will be to new climatic and land-use scenarios, we must improve our knowledge of dieback processes by integrating and analysing the roles played by these less-studied factors.

In this study, we carried out a comprehensive assessment of forest dieback causes (climate and drought stresses, competition and fungal pathogens) in three silver fir

103 (*Abies alba*) Pyrenean stands: one managed site that had been subjected to changes in

104 forest structure in the past and two unmanaged sites located within a National Park

105 where no logging had occurred for the past 50 years. Silver fir dieback has been an

106 ongoing process in the western Pyrenees since the 1980s (Camarero et al., 2011).

107 Previous studies have evaluated different drivers involved in the silver fir dieback

108 events and mostly focused either on the roles played by droughts (Linares and

109 Camarero, 2012) or by fungal pathogens (Oliva and Colinas, 2007). However, in this

110 study, we performed a multifactorial assessment of potential drivers of silver fir dieback

111 and their interactions with forest structure. We used new techniques that enabled

112 comparing the past radial growth of declining and non-declining silver fir trees showing

113 different levels of defoliation, here used as a proxy of vigour. Specifically, (i) we

114 reconstructed and analysed the growth patterns and trends and their responses to climate

115 in declining and non-declining silver fir trees; (ii) we then related those growth patterns

116 to several factors to determine their roles as drivers of dieback. We hypothesized that

117 drought triggers dieback (inciting factor *sensu* Manion, 1991), whereas past-use

118 predisposes trees to decline and fungal pathogens contribute to final tree death. In

119 particular, we expected that: trees with more severe defoliation and recently dead trees

120 would show the lowest growth rates, their growth patterns would be most sensitive to

121 drought, they would be subjected to the highest competition levels and that fungal

122 pathogens would be detected frequently in their wood. Since climate models forecast

123 warmer and drier conditions, dieback processes could become more widespread,

124 affecting temperate forests such as Pyrenean silver fir stands. This study aims to

125 improve the knowledge on the roles played by dieback agents so as to evaluate the

126 vulnerability of the silver fir populations and similar temperate conifer forests.

127

128   **2. Material and methods**

129   *2.1. Study sites*

130   The three study sites were located in northern Aragón in the central-western Spanish

131   Pyrenees (Fig. 1, Table 1). The sites are three silver fir (*Abies alba* Mill.) stands located

132   near the south-western limit of the distribution of the species. Here, silver fir usually

133   grows in mesic sites on north-facing slopes, forming pure or mixed forests with

134   European beech (*Fagus sylvatica* L.) or Scots pine (*Pinus sylvestris* L.). All stands were

135   situated on deep and basic soils and formed mixed forests. The understory vegetation

136   was dominated by European box (*Buxus sempervirens* L.). Three silver fir stands

137   characterized by abundant dominant trees with high levels of defoliation were selected

138   (Table 2). Given that we were interested in comparing silver fir stands with diverse

139   historical management, we selected one site (Paco Ezpela) with signs that intense

140   logging activity had been undertaken in the past (abundant stumps and wood trails) and

141   two sites (Cotatuero and Turieto) that had not been logged for at least the past 50 years

142   located in the "Ordesa y Monte Perdido" National Park, where strict conservation

143   policies have been followed since the establishment of the park in 1918 (Fig. 1). Both

144   unmanaged sites present different topographical and structural features (Table 1).

145   Furthermore, Cotatuero is a mixed forest with Scots pine, whereas in Turieto European

146   beech is more abundant. According to meteorological data, the climate in the study area

147   is continental, with a relatively cool and wet summer and annual precipitation varies

148   between 1153 mm (Paco Ezpela site) and 1326 mm (Turieto and Cotatuero sites) (see

149   Supplementary Material, Fig. S1).

150

151   *2.2. Climate data and drought index*

152 We obtained long-term (1900–2012) monthly climatic variables (mean maximum and

153 minimum temperatures and total precipitation) from the Climate Research Unit TS3.1

154 database, which provided homogenized and quality-controlled data at 0.5° spatial

155 resolution for the three study sites (Harris et al., 2014). The data were downloaded using

156 the Koninklijk Nederlands Meteorologisch Instituut Climate Explorer

157 (http://climexp.knmi.nl).

158   To estimate the effect of drought intensity on tree growth, we used the standardized

159 precipitation-evapotranspiration index (SPEI), which is a multi-scalar drought index

160 with negative and positive values corresponding to dry and wet periods, respectively

161 (Vicente-Serrano et al., 2010). The SPEI values for the period 1900–2011 were also

162 obtained with a 0.5° spatial resolution from the Global SPEI database

163 (http://sac.csic.es/spei/index.html). We selected the August 4-month SPEI values (i.e.

164 the August SPEI for drought accumulated up to 4 months before) as the best indicator of

165 drought stress for silver fir growth following Pasho et al. (2011). According to the SPEI,

166 the three driest years in the past 25 years were 1986, 1995 and 2005.

167

168 *2.3. Field sampling and dendrochronological methods*

169 Tree-ring width data were used to reconstruct past growth trends (Fritts, 2001), whilst

170 recent crown cover was regarded as a proxy of tree vigour (Dobbertin, 2005). Field

171 sampling was carried out in the autumns of 2011 and 2012. Following the

172 dendrochronological standards, at each site at least 30 dominant or co-dominant

173 standing silver fir trees were randomly selected across an area of 0.5-ha (15 non-

174 declining and 15 declining trees). For each sampled tree, the proportion of crown cover

175 was estimated to the nearest 5% (Schomaker et al., 2007). Given that estimates of the

176 proportion of crown cover tend to vary among observers and places, the data were

always recorded by the first author, who compared every tree with a reference tree with the maximum amount of foliage at each site. Non-declining trees were considered those with a crown cover of $> 50\%$ and declining trees those with a crown cover of $\leq 50\%$ (Camarero et al., 2015). Other classification types of vitality based on different crown cover thresholds (40% or 60%) produced similar results (Supplementary Material, Fig. S2). Trees that were either completely defoliated or that retained only red needles were considered to be 'recently dead'. Data obtained for declining and dead trees were grouped together in further analyses given that they presented similar growth trends (Supplementary Material, Fig. S3).

Two cores were taken from each tree at a height of 1.3 m (diameter at breast height, dbh) using a Pressler increment borer. In total, 142 trees were cored, corresponding to 64 non-declining trees and 78 declining trees (see Table 1 for site values). The wood samples were air-dried and polished with a series of successively finer sand-paper grits until the tree-rings were clearly visible. Afterwards, the wood samples were visually cross-dated and measured to the nearest 0.01 mm using a binocular microscope and a LINTAB measuring device (Rinntech, Heidelberg, Germany). The cross-dating process was checked and verified using the program COFECHA (Holmes, 1983). Pith-offset estimations were calculated fitting a geometric pith locator to the innermost rings. For the oldest trees, tree age at 1.3 m was estimated by counting the rings in the core of living trees and adding the estimate length of core missing up to the predicted pith. The age structure of the codominant and dominants trees was reconstructed in the three sites (Supplementary Material, Fig. S4). Finally, relative positive growth changes were calculated between 1940 and 2000 to detect releases associated with past thinning (Supplementary Material, Fig. S5). Growth changes were calculated calculating ring-width medians for 10-year periods following Nowacki and Abrams (1997). Releases

202   were regarded as periods with at least five consecutive years showing positive growth

203   changes greater than 50%.

204   We transformed tree-ring width into basal area increment (BAI), which is a more

205   biologically meaningful descriptor of growth trends than tree-ring width (Biondi and

206   Qaedan, 2008). The BAI was calculated from tree-ring widths as the difference between

207   consecutive cross-sectional basal areas (*BA*) estimated for years *t*+1 and *t* as:

208    $$BAI_{t+1} = BA_{t+1} - BA_t = \pi \left(\left(CL_t + TRW_{t+1} \right)^2 - \left(CL_t \right)^2 \right) \qquad (1),$$

209   where *CL* is the core length and *TRW* is the tree-ring width corresponding to years *t*+1

210   and *t*. Finally, we compared non-declining and the declining BAI series using Student *t*-

211   tests.

212

213   *2.4. Long-term BAI trends*

214   We used generalized additive mixed models (GAMMs; Wood, 2006) to compare the

215   long-term BAI trends of declining and non-declining trees. GAMM is a flexible semi-

216   parametric method of characterizing non-linear relationships, such as those observed

217   between the response variable (i.e. BAI), and one or several explanatory variables, such

218   as tree age or time (Augustin et al., 2009). Given that BAI depends on site conditions as

219   well as on the particular growth conditions to which each individual tree is subjected

220   during its life (e.g., Pokharel and Froese, 2009), we used GAMMs to describe growth

221   trajectories of coexisting non-declining and declining trees while controlling for the

222   influence of specific tree factors such as tree age and size (dbh). The GAMM we fitted

223   was of the form:

224    $$BAI_i = s(dbh_i) + s(tree\ age_i) + s(calendar\ year) + Z_i B_i + \upsilon_i \qquad (2),$$

225   where the BAI of tree *i* (BAI_i) is modelled as smooth functions (*s*) of three predictor

226   variables (dbh, tree age and calendar year). To take into account each individual tree

227 and site, tree identity (Z_iB_i) was considered as a random effect. In this and subsequent

228 analyses we also included an error term (v_i) with an AR1 (p=1, q=0) correlation

229 structure in the model to account for the first-order temporal autocorrelation of BAI.

230 The smooth terms were represented using thin plate regression splines (Wood, 2006).

231 The degree of smoothness was determined by internal cross validation during the fitting

232 process (Wood, 2003). Calendar year was considered as a covariate representing how

233 the tree ages from its establishment to the date on which the core was extracted (i.e.

234 cambial age), and tree age was entered as a fixed value representing the age of the tree.

235 We calculated GAMMs using the *mgcv* package (Wood, 2011).

236

237 *2.5. Competition index*

238 To quantify the potential effect of recent tree-to-tree competition on dieback, we

239 calculated a distance-dependent competition index (CI) for the three study sites. To

240 achieve this, we used a recently developed device that enables all the trees located up to

241 15 m away from the device to be mapped and their sizes estimated (see Rodríguez-

242 García et al., 2014). The device consists of a pair of stereoscopic cameras with fisheye

243 lenses and parallel optical axes, which enables hemispherical photographs to be taken at

244 a height of 1.2 m above the ground. The images are processed with specifically

245 designed image analysis software and validated against field measurements, enabling

246 the dbh, total height and the relative position of each neighbouring tree to the focal tree

247 located near the device to be obtained. We considered all the tree species in the study

248 area. At each site, at least 20 dominant or co-dominant cored silver fir trees (10 non-

249 declining and 10 declining trees per site) were randomly selected to determine the CI

250 within a 15-m radius of each focal tree. The CI of focal tree *i* was calculated taking into

251 account the number, dbh and distance to the neighbouring trees as follows:

252
$$\text{CI} = \sum_{j=1}^{n(R)} \left(\frac{\dfrac{dbh_j^2}{dbh_i^2}}{dist_{ij}} \right) \qquad (3),$$

253   where dbh_i and dbh_j are the dbh measurements for the focal tree i and neighbouring

254   trees, respectively, and $dist_{ij}$ is the distance separating them. The CI was calculated for

255   all neighbouring trees within a radius of $R \leq 15$ m from tree i except where the radius

256   overlapped the plot borders.

257

258   *2.6. Linear mixed-effects models of BAI*

259   To test whether trees with contrasting vigour show different growth responses to several

260   drivers (e.g., climate), linear mixed-effects models were separately fitted to BAI data of

261   non-declining and declining trees for the three study sites considering the period 1950–

262   2011. We adjusted the following linear mixed-effects model:

263
$$BAI_i = X_i\beta + Z_i b_i + \varepsilon_i \qquad (4),$$

264   where BAI_i represents the growth of tree i, and β is the vector of fixed effects (climate

265   variables, SPEI and competition index), b_i is the vector of random effects (tree age), X_i

266   and Z_i are fixed and random effects regressor matrices, and ε_i is the within group error

267   vector. We log(x+1)-transformed BAI in this and the following analyses because it

268   tended to have a skewed distribution.

269   We used selected seasonal temperature and precipitation data as climatic predictors

270   of BAI according to previous works (Camarero et al., 2011; Pasho et al., 2011). We

271   considered the following seasons: previous autumn (September to November) and

272   winter (December to February), and the spring (March to May) and summer (June to

273   August) of the year of tree-ring formation. The CI and the 4-month August SPEI values

274   were also used as BAI predictors. Residuals of the models were checked for normality,

275   homoscedasticity and temporal autocorrelation. The effects of climate, drought and CI

276   on BAI were tested and compared with a null model considering BAI as a constant. We

277   also evaluated the existence of multicollinearity among fixed effects by calculating the

278   variance inflation factor, which was always lower than three, suggesting no redundancy

279   problems among predictors (Zuur et al., 2009). We used an information-theoretic

280   approach for multi-model selection based on minimizing the Akaike information

281   criterion corrected for small sample sizes (AICc) (Burnham and Anderson, 2002). We

282   also calculated the difference in AICc between each model and the best one (*Δi*), and

283   the relative probability that model *i* was the best one for the observed data (*Wi*). We

284   considered models with substantial support to be those in which the Δ*AICc* between

285   models was less than two (Zuur et al., 2009). We fitted linear mixed-effects models

286   using the *nlme* package (Pinheiro and Bates, 2000). All statistical analyses were

287   performed using the R statistical software (R Development Core Team, 2013).

288

289   *2.7. BAI responsiveness to drought*

290   We evaluated the effect of drought stress on growth based on the relative changes in

291   BAI for three selected drought years (1986, 1995 and 2005) showing the lowest SPEI

292   values for the past 25 years (Supplementary Material, Fig. S1). We defined drought

293   sensitivity (*DS*) and drought recovery (*DR*) based on the relative changes in BAI for the

294   three selected drought years as follows (see Linares and Tíscar, 2010; Sangüesa-Barreda

295   et al., 2012):

296 $$DS = \left[\frac{(BAI_D - BAI_{D-s})}{BAI_{D-s}}\right] \times 100 \qquad (5)$$

297 $$DR = \left[\frac{(BAI_{D+s} - BAI_{D-s})}{BAI_{D-s}}\right] \times 100 \qquad (6),$$

298   where BAI_D is the BAI value for the drought year, BAI_{D-3} is the mean BAI for the three

299   years before the drought year and BAI_{D+3} is the mean BAI for the three years after the

300   drought occurred. The three-year interval was selected because it adequately reflects the

301   short-term effects of drought on BAI changes (Sangüesa-Barreda et al., 2012).

302

303   *2.8. Fungal pathogens inhabiting stem and root wood*

304   Previous studies of silver fir decline have detected the presence of the root-rot

305   pathogens *Armillaria* and *Heterobasidion* species (Oliva and Colinas, 2007, 2010). To

306   detect the presence of fungal pathogens inhabiting stem and root wood that could be

307   linked to dieback and tree death, we extracted two cores per tree from the tree base and

308   also from the coarse roots in November 2012. In total, 50 declining and 25 non-

309   declining trees were analyzed (30 trees in Cotatuero and 45 in Paco Ezpela). The wood

310   cores were placed in sterile plastic tubes and then, within three days of sampling, plated

311   onto a malt-extract-based selective media for basidiomycetes that included benomyl (10

312   mg l^{-1}) and chloramphenicol (200 mg l^{-1}). Cores were incubated at 20–22°C in the dark

313   and observed weekly for three months. Fungal colonies that grew out from the cores

314   were transferred onto malt agar plates. To identify the fungal isolates, DNA was

315   extracted, the internal transcribed spacer region was amplified, sequenced and BLAST

316   searches were performed using the GenBank and UNITE databases (Benson et al.,

317   2013; Kõljalg et al., 2005). A similarity threshold of 98% was used for typing the

318   sequences at species level. We compared the observed and expected (equal numbers of

319   fungi present irrespective of decline status) number of trees in which the most abundant

320   fungi were present using the χ^2 statistic, applying the Yates' correction (Agresti, 1990),

321   and considering only fungal species isolated in more than two trees for all the sites

322   combined. Lastly, we studied the BAI trends of trees hosting the main fungal species in

323   the managed Paco Ezpela and the unmanaged Cotatuero sites since 1970 because fungal

324   pathogens were found in more trees at these two sites than in Turieto. Hence, we

325   combined and grouped trees at Paco Ezpela and Cotatuero to obtain a robust sample size

326   of each class: non-declining trees, declining trees without fungal pathogens, declining

327   trees colonized by the primary fungal pathogen *Heterobasidion* spp. and declining trees

328   colonized by the secondary fungal pathogen *Amylostereum chailletii*.

329

330   **3. Results**

331   *3.1. Characteristics of non-declining and declining silver fir trees*

332   Among the three sites investigated in this study, the managed site Paco Ezpela showed

333   the most severe dieback in terms of number of declining trees (Table 1). In addition,

334   Paco Ezpela showed the highest frequency of trees presenting releases associated to past

335   thinning (Supplementary Material, Fig. S5).There was no significant difference between

336   non-declining and declining trees with regards to tree age, dbh or CI at the three study

337   sites (Table 2), except for the managed Paco Ezpela site where the non-declining trees

338   had a significantly bigger dbh than the declining trees. Significant differences were

339   detected in the current crown cover and the BAI of the last 10 years. A comparison of

340   stand characteristics between sites revealed that the CI was significantly higher at the

341   unmanaged Turieto site than elsewhere.

342

343   *3.2. BAI divergence between non-declining and declining trees*

344   Declining trees showed a lower BAI than non-declining trees over the past two decades.

345   Indeed, the difference in BAI between non-declining and declining trees began in the

346   late 1980s in Paco Ezpela and Cotatuero, whereas in Turieto this trend started in the late

347   1990s (Fig. 2). In Turieto, a severe reduction in growth occurred between 1994 and

1997, which was associated with an outbreak of the Lepidoptera *Epinotia subsequana* Hw, which resulted in severe defoliations. Both declining and non-declining trees recovered BAI rates after the defoliation, with declining trees showing lower growth rates than non-declining trees. Significantly lower BAI values were observed for declining than for non-declining trees between 2001 and 2012 at the Cotatuero and Paco Ezpela sites ($P < 0.05$), and this was also detected at the site in Turieto in some years during the 2000s. In addition, in Turieto declining trees showed higher BAI values than non-declining trees between 1925 and 1965.

We did not find significant differences in terms of drought sensitivity and recovery, i.e. relative changes in BAI, between non-declining and declining trees (Supplementary Material, Fig. S6), excepting a significantly lower level of drought recovery in declining trees compared with that of non-declining trees in Cotatuero (unmanaged site) and Paco Ezpela (managed site) in response to the 2005 drought (Supplementary Material, Fig. S6).

3.3. Long-term growth patterns

The best-fit GAMMs considered the calendar year, as well as tree age and dbh, with significant effects on BAI in all the cases, except in some cases of tree age for declining and non-declining trees in several sites (Table 3). In Cotatuero, the divergent growth patterns of declining and non-declining trees have been accentuated since the severe reduction in growth in 1986, and declining trees showed higher BAI values than non-declining trees from the 1940s to the 1960s (Fig. 2). In Turieto, BAI trends of non-declining and declining trees were similar but declining trees always showed higher growth rates. However, the GAMMs were unable to model the severe post-outbreak reduction of BAI in the declining trees described before. Finally, at the managed Paco

373   Ezpela site, declining trees had lower BAI values than non-declining trees throughout

374   the 20th century and both tree types showed a notable reduction in BAI in the 1980s.

375

376   *3.4. Roles played by climatic variables in the dieback process.*

377   The linear mixed-effects models showed that the most significant drivers of BAI were

378   August SPEI (wet and cool summer conditions enhance growth) and winter minimum

379   temperatures and precipitation (cold and wet previous winter conditions reduce growth)

380   (Table 4; see also Supplementary Material, Table S1). In Paco Ezpela, the BAI was also

381   positively affected by the spring maximum temperatures and the previous autumn

382   precipitation. At all three study sites, BAI was negatively affected by the CI,

383   particularly in the case of declining trees growing in Cotatuero and Paco Ezpela and

384   non-declining trees growing in Turieto. Models considering climatic variables and

385   competition explained the BAI better at the managed site (higher *Wi* values in Table 4)

386   than at the two unmanaged sites.

387

388   *3.5. Fungal pathogens and BAI trends*

389   The secondary fungal pathogen *Amylostereum chailletii* was isolated from eight

390   declining silver firs, which was a frequency significantly higher than expected (Table

391   5). Declining and non-declining trees also hosted *Heterobasidion annosum* or

392   *Trichaptum abietinum* at frequencies that were not different from random expectation.

393   Trees hosting the primary fungal pathogen *Heterobasidion* showed a sharp decline in

394   BAI from 2007 onwards until reaching growth rates that were as low as declining trees

395   (Fig. 3), whereas trees hosting *A. chailletii* showed a moderate reduction in BAI from

396   the early 2000s onwards.

397

4. Discussion

Our study of managed and unmanaged silver fir stands has revealed the different roles played by dieback-causing factors. We were able to assess the relative importance of the evaluated factors in silver fir dieback. The retrospective growth information provided by the tree-ring data revealed that there had been a sharp reduction in BAI since 1986, a year characterized by a severe late-summer drought stress (Fig. 2). The declining trees of the managed site, characterized by a long history of use (logging), showed persistently low growth rates. On the other hand, we did not find a high number of declining trees infested by primary pathogens, but we detected a higher number of trees infested by *Amylostereum* sp. than expected (Table 5). Growth patterns indicate showed that trees infested by *Heterobasidion* sp. or *Amylostereum* sp. presented lower growth than non-declining trees (Fig. 3).

The stands investigated have been subjected to different management history and our findings reveal the role that logging has played in predisposing trees to dieback. Past logging in the disturbed and formerly managed sites has resulted in the negative selection of slow-growing and smaller trees with show a high level of vulnerability to drought and a high sensitivity to water deficit and competition. By contrast, at unmanaged sites, the recent droughts have affected trees irrespective of the past logging in their neighborhood. This was demonstrated by the greater differences in the growth patterns of declining and non-declining trees (Fig. 2) and their responses to climate (Table 4) when comparing the formerly logged or managed site (Paco Ezpela) with the unlogged sites (Cotatuero and Turieto). These findings demonstrate that the impact of climate warming on forests cannot be fully understood without a proper understanding of historical land use and the interplay between past legacies and current climatic stressors such as droughts.

423   The most important differences between non-declining and declining trees in terms

424   of BAI responses to drought and BAI trends after the 1986 drought were found at the

425   managed Paco Ezpela site (see Fig. 2). This stand illustrates how past logging has

426   affected the dynamics of most Spanish Pyrenean forests as a result of intensive forest

427   use between the 1950s and the 1970s (Cabrera, 2001; Camarero et al., 2011). Such past

428   intensive logging have led to a negative selection of trees by cutting the biggest trees

429   with the fastest growth rates and promoting the persistence of the smallest and slowest

430   growing trees, some of which had a poor ability to cope with dry conditions. Our

431   findings concur with this view given that non-declining trees had a greater diameter

432   than non-declining trees at this site (Table 2). Furthermore, this result can be applied to

433   the other Pyrenean stands subjected to ongoing dieback given that they are characterized

434   by trees with smaller diameter than stands with asymptomatic trees irrespective of site

435   conditions and tree age (Camarero et al., 2011). Alternatively, logging could have

436   modified the microclimatic conditions of affected forests by creating abundant gaps and

437   increasing vapour pressure deficit near the canopy, which is known to adversely affect

438   silver fir performance and increase its vulnerability to drought (Aussenac, 2002). Our

439   findings agree with previous studies showing that drought causes dieback and that past

440   management synergistically predisposes trees to be more vulnerable to water deficit

441   (Reams and Huso, 1990). Other studies in subalpine forests have also highlighted the

442   high risk of mortality in trees with reduced pre-drought radial growth rates (Bigler et al.,

443   2007). Lastly, the historical logging regime could have increased the density of stumps

444   acting as dispersion foci for *Heterobasidion* species, leading to dieback and higher

445   levels of root-rot infection. In unmanaged forests, it is also possible that fallen,

446   uprooted, and dead trees act as dispersion foci of fungal pathogens, but we consider this

447   occurs in a much lower incidence than in managed sites with abundant stumps and

448 dying trees. However, this idea requires additional testing because we did not detect

449 *Heterobasidion* species in all declining trees (Table 5). Overall, we consider past

450 logging and drought to be predisposing and inciting factors, respectively, in the

451 conceptual framework of dieback proposed by Manion (1991).

452 The results confirmed the major importance of the cumulative late-summer water

453 deficit on BAI of silver fir (Table 4), and that this is the stressor that is particularly

454 relevant for silver fir in drought-prone European populations (Macias et al., 2006;

455 Carrer et al., 2010; Linares and Camarero, 2011). In silver fir, warm temperatures and

456 periods of protracted water shortage negatively affect primary growth and carbon

457 synthesis in late summer prior to growth through rising vapour pressure deficit

458 (Aussenac, 2002). If very warm conditions lead to reduced soil water reserves and

459 severe drought, dieback occurs and it is manifested through a rapid decline in growth

460 and fast defoliation, leading to tree death, or an increase in the vulnerability of affected

461 stands against further stressors (Galiano et al., 2010; Camarero et al., 2014). Our results

462 concur with this view given that we found a reduction in the capacity of declining trees

463 to recover BAI after severe droughts (Supplementary Material, Fig. S6). This was mots

464 evident in response to the most recent drought, which suggests that droughts have an

465 accumulative negative effect on growth and performance.

466 In the case of trees at the Turieto site, the BAI decline occurred after the *E.*

467 *subsequana* outbreak, which had already been documented in several Pyrenean silver fir

468 forests (Camarero et al., 2003). Silver firs at the Turieto site responded more slowly to

469 drought stress and were less affected than at the other sites because the Turieto site is a

470 north-facing mesic site with well-developed soils and a high capacity to hold water

471 (Supplementary Material, Fig. S6). This could also explain the high basal area recorded

472 for trees growing in Turieto and the low number of dead trees (Table 1). In addition,

473   declining trees grew better than non-declining trees at that site (Figs 2); however, they

474   were less adapted to withstand the warm and dry 1990s and 2000s, perhaps owing to the

475   production of drought-vulnerable tracheids with ample lumens or the formation of less-

476   developed root systems (see Voltas et al., 2013).

477   The long-term BAI patterns differed for non-declining and declining silver firs at the

478   Cotatuero and Paco Ezpela sites even though the declining silver firs at both sites

479   showed a similar decrease in BAI after the 1986 drought (Figs 2). The comparison of

480   observed and modelled BAI trends indicates that this decline in BAI was recent and

481   triggered by drought in Cotatuero, whereas declining trees in Paco Ezpela had shown

482   low growth rates since the 1950s when logging intensified. In both cases, the BAI

483   differences between the declining classes magnified in the 2000s, which has also been

484   observed in other stands showing dieback (Linares and Camarero, 2012a).

485   The current competition levels between declining and non-declining trees were not

486   significantly different (Table 2), which agrees with previous findings in the Pyrenees

487   (Camarero et al., 2011) but contrasts with observations from silver fir forests in the

488   Vosges (Becker et al., 1989) or Mediterranean pinsapo fir stands in southern Spain

489   (Linares et al., 2010) where dieback was linked to high competition in drought-prone

490   areas. However, the linear mixed-effects models of BAI confirmed that current

491   competition negatively drove growth in declining trees in Paco Ezpela but also in non-

492   declining trees in Turieto (Table 4). This suggests that the current competition levels

493   explain part of the recent growth trends at local scales but does not always imply

494   dieback. However, we need more data on recently dead trees from additional sites to

495   determine the influence of any sampling effect on this result. Furthermore, the relevance

496   of the understory vegetation as a source of competition for soil water should be better

497   evaluated.

498   Silver fir dieback in the three stands investigated in this study cannot be ascribed to

499   the presence of particular fungal pathogens because a high proportion of the declining

500   trees were not infected by primary pathogens but by the secondary pathogens *A.*

501   *chailletii* and *T. abietinum* (Table 5). We mainly detected primary fungal pathogens

502   (mostly *H. annosum*) that infected and eventually may kill vigorous trees (Korhonen

503   and Stenlid, 1998), and secondary or opportunistic fungal pathogens (mainly *A.*

504   *chailletii*) that usually attack already weakened, stressed or wounded trees (Slippers et

505   al., 2003). Only in the case of secondary pathogens was the proportion of trees infected

506   significantly higher than expected, indicating a higher incidence of *A. chailletii* in

507   declining trees. Overall, our findings indicate that the fungi inhabiting the wood are not

508   the main cause of the silver fir dieback process but merely act as contributing factors

509   (*sensu* Manion 1991), as previously noted by Oliva and Colinas (2007). Moreover, we

510   found different BAI patterns as a function of the presence of different fungal pathogens

511   (Fig. 3). Trees hosting the primary fungal pathogen *Heterobasidion* spp. showed an

512   abrupt decrease in BAI, probably in response to a recent but severe infection process,

513   which agrees with previous findings showing that *H. annosum* is able to cause rapid and

514   sharp declines in growth in previously dominant or fast-growing trees (Cherubini et al.,

515   2002). By contrast, trees hosting the secondary fungal pathogen *A. chailletii* showed a

516   long and gradual decline in BAI. The BAI patterns of silver firs infected by primary

517   fungal pathogens reflect a long-term infection process in which carbon pools are mainly

518   diverted towards defence rather than growth and wood formation (Oliva et al., 2014).

519   However, trees with secondary pathogens showed high BAI values in the past followed

520   by a recent decline in their growth, probably in response to droughts in the 2000s, which

521   suggests that fungi-infested trees have a high level of vulnerability to drought.

522   We have assessed the roles played by several dieback agents such as drought,

523   current competition and presence of fungal pathogens using BAI trends and defoliation

524   as response variables or indicators of tree growth and vigour. However, our

525   retrospective approach and the observational nature of our data do not allow the

526   temporal evolution and changes in the relevance of all those dieback causal agents to be

527   detected except for drought. Nonetheless, we consider that the current growth and

528   defoliation conditions of trees reflect the last years of the dieback process. Furthermore,

529   dendrochronological data have enabled the long-term changes in tree vigour in

530   numerous dieback studies to be quantified (see Wunder et al., 2008). However,

531   additional limitations must be considered. First, we are aware that future studies should

532   include more sites and trees to properly disentangle the interacting effects of various

533   environmental (drought, pathogens) and human-related (logging) drivers on forest

534   dieback, i.e. to increase the inferential strength of the presented findings. Second, there

535   are temporal lags between the stressor (e.g., drought) and the tree responses (BAI

536   decline, defoliation) and there can also be a time lag between those responses of up to

537   several decades (Bigler and Rigling, 2013). Third, we cannot reconstruct the long-term

538   changes in the abundance of fungal pathogens inhabiting wood but only detect their

539   current presence. The findings relating to fungal pathogens must also be interpreted

540   with caution because a substantial proportion of the fungal infection may have gone

541   undetected by sampling in the stem and coarse roots and not in the root system. Lastly,

542   cumulative or 'memory' effects of successive and interactive stressors (e.g., recurrent

543   droughts) are difficult to pinpoint without additional indicators such as carbon isotopes

544   (Linares and Camarero, 2012b).

545   To conclude, ongoing dieback processes triggered by drought are threatening some

546   Pyrenean silver fir stands at the southernmost distribution limit of the species. The

547 dieback is characterized by a rapid defoliation and a sharp growth decline after severe

548 late-summer droughts. Although past logging activities at the managed sites may have

549 predisposed the trees at these sites to dieback, trees at unmanaged sites also showed

550 signs of dieback irrespective of the current competition levels and the presence of

551 primary fungal pathogens. If climatic conditions become warmer and drier in the future,

552 dieback processes will become more widespread, affecting more silver fir stands, which

553 would favour vegetation shifts to mixed forests dominated by tree species better adapted

554 to drought such as Scots pine.

555

562

References

Adams, H.D., Guardiola-Claramonte, M., Barron-Gafford, G.A., Villegas, J.C., Breshears, D.D., Zou, C.B., Troch, P.A., Huxman, T.E., 2009. Temperature sensitivity of drought-induced tree mortality portends increased regional die-off under global-change-type drought. Proc. Natl. Acad. Sci. U.S.A. 106, 7063–7066.

Agresti, A., 1990. Categorical Data Analysis. Wiley, New York.

Allen, C.D., Macalady, A.K., Chenchouni, H., Bachelet, D., McDowell, N., et al., 2010. A global overview of drought and heat-induced tree mortality reveals emerging climate change risks for forests. Forest Ecol. Manag. 259, 660–684.

Augustin, N.H., Musio, M., von Wilpert, K., Kublin, E., Wood, S.N., Schumacher, M.. 2009. Modeling spatiotemporal forest health monitoring data. J. Am. Stat. Assoc. 104, 899–911.

Aussenac, G., 2002. Ecology and ecophysiology of circum-Mediterranean firs in the context of climate change. Ann. For. Sci. 59, 823–832.

Ayres, M.P., Lombardero, M.J., 2000. Assessing the consequences of global change for forest disturbance from herbivores and pathogens. The Science of the Total Environment 262, 263–86.

Becker, M., Landmann, G., Levy, G., 1989. Silver fir decline in the Vosges mountains (France): role of climate and silviculture. Water, Air and Soil Pollution 48, 77–86.

Benson, D.A., Cavanaugh, M., Clark, K., Karsch-Mizrachi, I., Lipman, D.J., Ostell, J., Sayers, E.W., 2013. GenBank. Nucleic Acids Res. 41, D36–D42.

Bigler, C., Bräker, O.U., Bugmann, H., Dobbertin, M., Rigling, A., 2006. Drought as an inciting mortality factor in Scots pine stands of the Valais, Switzerland. Ecosystems 9, 330–343.

587   Bigler, C., Gavin, D.G., Gunning, C., Veblen, T.T., 2007. Drought induces lagged tree

588   mortality in a subalpine forest in the Rocky Mountains. Oikos 116, 1983–1994.

589   Bigler, C., Rigling, A., 2013. Precision and accuracy of tree-ring-based death dates of

590   mountain pines in the Swiss National Park. Trees 27, 1703–1712.

591   Biondi, F., Qeadan, F., 2008. A theory-driven approach to tree-ring standardization:

592   defining the biological trend from expected basal area increment. Tree-Ring

593   Research 64, 81–96.

594   Bonan, G.B., 2008. Forests and climate change: forcings, feedbacks, and the climate

595   benefits of forests. Science 320, 1444–1449.

596   Burnham, K.P., Anderson, D.R., 2002. Model Selection and Multimodel Inference.

597   Springer-Verlag, New York.

598   Cabrera, M., 2001. Evolución de abetares del Pirineo aragonés. Cuadernos de la

599   Sociedad Española de Ciencias Forestales. 11, 43–52.

600   Cailleret, M., Nourtier, M., Amm, A., Durand-Gillmann, M., Davi, H., 2014. Drought-

601   induced decline and mortality of silver fir differ among three sites in Southern

602   France. Annals of Forest Science 71, 643–657.

603   Camarero, J.J., Martín-Bernal, E., Gil-Pelegrín, E., 2003. The impact of a needle miner

604   (*Epinotia subsequana*) outbreak on radial growth of silver fir (*Abies alba*) in the

605   Aragón Pyrenees: A dendrochronological assessment. Dendrochronologia 21, 1–10.

606   Camarero, J.J., Bigler, C., Linares, J.C., Gil-Pelegrín, E., 2011. Synergistic effects of

607   past historical logging and drought on the decline of Pyrenean silver fir forests.

608   Forest Ecol. Manag. 262, 759–769.

609   Camarero, J.J., Gazol, A., Sangüesa-Barreda, G., Oliva, J., Vicente-Serrano, S.M.,

610   2015. To die or not to die: early warnings of tree dieback in response to a severe

611   drought. Journal of Ecology 103, 44–57.

612   Carrer, M., Nola, P., Motta, R., Urbinati, C., 2010. Contrasting tree-ring growth to

613   climate responses of *Abies alba* toward the southern limit of its distribution area.

614   Oikos 119, 1515–1525.

615   Cherubini, P., Fontana, G., Rigling, D., Dobbertin, M., Brang, P., Innes, J.L., 2002.

616   Tree-life history prior to death: two fungal root pathogens affect tree-ring growth

617   differently. Journal of Ecology 90, 839–850.

618   Dobbertin, M., 2005. Tree growth as indicator of tree vitality and of tree reaction to

619   environmental stress: a review. European Journal of Forest Research 124, 319–333.

620   Dobbertin, M., Wermelinger, B., Bigler, C., Bürgi, M., Carron, M., Forster, B., Gimmi,

621   U., Rigling, A., 2007. Linking increasing drought stress to Scots pine mortality and

622   bark beetle infestations. The Scientific World Journal 7, 231–9.

623   Fritts, H.C., 2001. Tree Rings and Climate. Blackburn Press, Caldwell, NJ.

624   Galiano, L., Martínez-Vilalta, J., Lloret, F., 2010. Drought-induced multifactor decline

625   of Scots pine in the Pyrenees and potential vegetation change by the expansion of

626   co-occurring oak species. Ecosystems 13, 978–991.

627   Harris, I., Jones, P.D., Osborn, T.J., Lister, D.H., 2014. Updated high-resolution grids of

628   monthly climatic observations - the CRU TS3.10 Dataset. International Journal of

629   Climatology 34, 623–642.

630   Holmes, R.L., 1983. Computer-assisted quality control in tree-ring dating and

631   measurement. Tree-Ring Bulletin 43, 68–78.

632   Kõljalg, U., Larsson, K.H., Abarenkov, K., Nilsson, R.H., Alexander, I.J., Eberhardt,

633   U., Erland, S., Høiland, K., Kjøller, R., Larsson, E., et al., 2005. UNITE: a database

634   providing web-based methods for the molecular identification of ectomycorrhizal

635   fungi. New Phytologist 166, 1063–1068.

636   Korhonen, K., Stenlid, J., 1998. Biology of *Heterobasidion annosum*. In: Woodward S,

637   Stenlid J, Karjalainen R, Hüttermann A eds. Heterobasidion annosum: Biology,

638   Ecology, Impact and Control, Wallingford, UK: CAB International, 43-70.

639   Linares, J.C., Camarero, J.J., 2011. Growth patterns and sensitivity to climate predict

640   silver fir decline in the Spanish Pyrenees. Eur. J. Forest Res. 131, 1001–1012.

641   Linares, J.C., Camarero, J.J., 2012a. Silver fir defoliation likelihood is related to

642   negative growth trends and high warming sensitivity at their southernmost

643   distribution limit. ISRN Forestry 2012, 1–8.

644   Linares, J.C., Camarero, J.J., 2012b. From pattern to process: linking intrinsic water-use

645   efficiency to drought-induced forest decline. Global Change Biol. 18, 1000-1015.

646   Linares, J.C., Camarero, J.J., Carreira, J.A., 2010. Competition modulates the adaptation

647   capacity of forests to climatic stress: insights from recent growth decline and death

648   in relict stands of the Mediterranean fir *Abies pinsapo*. Journal of Ecology 98, 592–

649   603.

650   Linares, J.C., Tíscar, P.A., 2010. Climate change impacts and vulnerability of the

651   southern populations of *Pinus nigra* subsp. *salzmannii*. Tree Physiol. 30, 795–806.

652   Macias, M., Andreu, L., Bosch, O., Camarero, J.J., Gutiérrez, E., 2006. Increasing

653   aridity is enhancing silver fir (*Abies alba* Mill.) water stress in its south-western

654   distribution limit. Clim. Change 79, 289–313.

655   Manion, P.D., 1991. Tree Disease Concepts. Prentice-Hall. Englewood Cliffs, NJ, USA.

656   McDowell, N.G., Ryan, M.G., Zeppel, M.J.B., Tissue, D.T., 2013. Feature: Improving

657   our knowledge of drought-induced forest mortality through experiments,

658   observations, and modeling. New Phytol. 200, 289–293.

659   Nowacki, G.J., Abrams, M.D., 1997. Radial-growth averaging criteria for

660   reconstructing disturbance histories from presettlement-origin oaks. Ecological

661   Monographs 67, 225–249.

662   Oliva, J., Colinas, C., 2007. Decline of silver fir (*Abies alba* Mill.) stands in the Spanish

663   Pyrenees: Role of management, historic dynamics and pathogens. Forest Ecol.

664   Manag. 252, 84–97.

665   Oliva, J., Colinas, C., 2010. Epidemiology of *Heterobasidion abietinum* and *Viscum*

666   *album* on silver fir (*Abies alba*) stands of the Pyrenees. Forest Pathology 40, 19–32.

667   Oliva, J., Stenlid, J., Martínez-Vilalta, J., 2014. The effect of fungal pathogens on the

668   water and carbon economy of trees: implications for drought-induced mortality.

669   New Phytol. 203, 1028–1035.

670   Oliva, J., Suz, L.M., Colinas, C.. 2009. Ecology of *Armillaria* species on silver fir

671   (*Abies alba*) in the Spanish Pyrenees. Ann. For. Sci. 66, 603.

672   Pasho, E., Camarero, J.J., De Luis, M., Vicente-Serrano, S.M., 2011. Impacts of drought

673   at different time scales on forest growth across a wide climatic gradient in north-

674   eastern Spain. Agric. For. Meteorol. 151, 1800–1811.

675   Pinheiro, J.C., Bates, D.M., 2000. Mixed-Effects Models in S and S-PLUS. Springer,

676   Berlin.

677   Pokharel, B., Froese, R.E., 2009. Representing site productivity in the basal area

678   increment model for FVS-Ontario. Forest Ecol. Manag. 258, 657–666.

679   Reams, G.A., Huso, M.M.P., 1990. Stand history: an alternative explanation of red

680   spruce radial growth reduction. Can. J. For. Res. 20, 250–253.

681   Rodríguez-García, C., Montes, F., Ruiz, F., Cañellas, I., Pita, P., 2014. Stem mapping

682   and estimating standing volume from stereoscopic hemispherical images. Eur. J.

683   Forest Res. 133, 895–904.

684   Sangüesa-Barreda, G., Linares, J.C., Camarero, J.J., 2012. Mistletoe effects on Scots

685   pine decline following drought events: insights from within-tree spatial patterns,

686   growth and carbohydrates. Tree Physiol. 32, 585–98.

687   Schomaker, M.E., Zarnoch, S.J., Bechtold, W.A., Latelle, D.J., Burkman, W.G., Cox,

688   S.M., 2007. Crown-Condition Classification : A Guide to Data Collection and

689   Analysis. Gen. Tech. Rep. SRS-102. Asheville, NC: U.S.D.A., Forest Service,

690   Southern Research Station. 78 p.

691   Slippers, B., Coutinho, T.A., Wingfield, B.D., Wingfield, M.J., 2003. A review of the

692   genus *Amylostereum* and its association with woodwasps. South African Journal of

693   Science 99, 70-74.

694   Van Mantgem, P.J., Stephenson, N.L., Byrne, J.C., Daniels, L.D., Franklin, J.F., Fulé,

695   P.Z., Harmon, M.E., Larson, A.J., Smith, J.M., Taylor, A.H., et al., 2009.

696   Widespread increase of tree mortality rates in the western United States. Science

697   323, 521–524.

698   Vicente-Serrano, S.M., Beguería, S., López-Moreno, J.I., 2010. A Multiscalar Drought

699   Index   Sensitive   to   Global   Warming: The   Standardized   Precipitation

700   Evapotranspiration Index. J. Clim. 23, 1696–1718.

701   Voltas, J., Camarero, J.J., Carulla, D., Aguilera, M., Ortiz, A., Ferrio, J.P., 2013. A

702   retrospective, dual-isotope approach reveals individual predispositions to winter-

703   drought induced tree dieback in the southernmost distribution limit of Scots pine.

704   Plant Cell Environ. 36, 1435–1448.

705   Williams, A.P., Allen, C.D., Macalady, A.K., Griffin, D., Woodhouse, C.A., Meko,

706   D.M., Swetnam, T.W., Rauscher, S.A., Seager, R., Grissino-Mayer, H.D., et al.,

707   2013. Temperature as a potent driver of regional forest drought stress and tree

708   mortality. Nat. Clim. Change 3, 292–297.

709   Wood, S.N., 2003. Thin-plate regression splines. Journal of the Royal Statistical Society

710   Series B 65, 95-114.

711   Wood, S.N., 2006. Generalized Additive Models: An Introduction with R. Chapman

712   and Hall/CRC, Boca Raton.

713   Wood, S.N., 2011. Fast stable restricted maximum likelihood and marginal likelihood

714   estimation of semiparametric generalized linear models. Journal of the Royal

715   Statistical Society Series B 73, 3-36.

716   Wunder, J., Reineking, B., Bigler, C., Bugmann, H., 2008. Predicting tree mortality

717   from growth data : how virtual ecologists can help real ecologists. Journal of

718   Ecology 96, 174–187.

719   Zhang, X., Lei, Y., Pang, Y., Liu, X., Wang, J., 2014. Tree mortality in response to

720   climate change induced drought across Beijing, China. Clim. Change 124, 179-190.

721   Zuur, A.F., Ieno, E.N., Walker, N., Saveliev, A.A., Smith, G.M., 2009. Mixed Effects

722   Models and Extensions in Ecology with R. Springer, NewYork.

723

724 **Figure captions**

725 **Figure 1.** (a) Geographical situation in the Spanish Pyrenees of the three silver fir

726 forests investigated in the study (CO, Cotatuero; TU, Turieto and PE, Paco Ezpela) and

727 the silver fir distribution in the Pyrenees and in the rest of Europe (green areas). The

728 blue line shows the limit of the Ordesa y Monte Perdido National Park. (b) Illustrative

729 views of trees showing dieback symptoms at the managed Paco Ezpela site (bottom left

730 and right images) and the unmanaged Cotatuero site (top right image).

731

732 **Figure 2.** Basal area increment (means ± SE) of non-declining trees (crown cover

733 >50%; green circles) and declining trees (crown cover ≤50%; red triangles) from 1900

734 to 2012 at the three study sites (Cotatuero, Turieto and Paco Ezpela). The bars indicate

735 the sampling depth (number of measured radii, colours are as indicated before). The

736 yellow box indicates the decline in growth between 1994 and 1997 due to defoliation

737 related to an *Epinotia subsequana* outbreak. The grey regions indicate years with

738 significant differences in basal area increment between non-declining and declining

739 trees. Furthermore, appear long-term basal area increment trends for declining (red

740 downward triangles) and non-declining (green circles) silver fir trees from three study

741 sites based on generalized additive mixed models.

742

743 **Figure 3.** Recent trends in basal area increment (means ± SE, lines with symbols) of

744 silver fir and annual sampling depth (number of measured radii, bars) of non-declining

745 trees (green upward triangles), declining trees without fungal pathogens (red downward

746 triangles), trees colonized by primary fungal pathogens such as *Heterobasidion* spp.

747 (blue circles) and trees colonized by secondary fungal pathogens such as *Amylostereum*

748   *chailletii* (yellow squares). Data corresponds to trees sampled in the unmanaged

749   Cotatuero and managed Paco Ezpela sites.

750

751 **Tables**

752 **Table 1.** Characteristics of the three silver fir sites

753 Non-declining and declining trees were defined as those with more than or less than or

754 equal to 50% crown cover, respectively.

755

Site (Code)	Latitude (N)	Longitude (W)	Aspect	Elevation (m a.s.l.)	Slope (°)	Basal area (m^2 ha^{-1})	No. trees	Percentage of non-declining / declining trees
Cotatuero (CO)	42º 39' 06''	0º 02' 36''	S-SW	1450	34	29.4	59	44 / 56
Turieto (TU)	42º 38' 51''	0º 04' 47''	N	1470	37	29.7	38	58 / 42
Paco Ezpela (PE)	42º 44' 25''	0º 49' 33''	N-NE	1170	27	15.1	45	36 / 64

756

757

758 **Table 2.** Features of the non-declining (>50% crown cover) and declining silver fir trees (≤50% crown cover) at the three study sites.

759 Different letters show significant differences (*P*<0.05) between non-declining and declining trees for each variable (Mann–Whitney tests).

760 Values are means ± SE.

761

Site (Code)	Tree type	No. trees (No. radii)	Dbh (cm)	Basal area increment (cm^2yr^{-1}) for the period 2002-2012	Age (years)	Crown cover (%)	No. trees used to calculate the competition index	Competition index
Cotatuero (CO)	Non declining	26 (49)	44.8 ± 3.4	14.3 ± 1.7b	115 ± 4	96.1 ± 1.8 b	17	2.86 ± 0.58
	Declining	33 (57)	45.3 ± 1.9	8.3 ± 1.0a	115 ± 11	16.8 ± 3.2 a	15	1.90 ± 0.25
Turieto (TU)	Non declining	22 (43)	34.2 ± 2.2	14.5 ± 1.6b	84 ± 4	98.2 ± 1.2 b	16	4.40 ± 0.66
	Declining	16 (31)	38.5 ± 2.0	6.7 ± 0.7a	88 ± 3	17.8 ± 3.3 a	8	4.86 ± 0.97
PacoEzpela (PE)	Non declining	16 (30)	40.3 ± 1.8b	21.6 ± 2.4b	90 ± 4	86.6 ± 2.6 b	10	2.53 ± 0.76
	Declining	29 (52)	34.2 ± 1.2a	8.2 ± 0.7a	92 ± 3	19.3 ± 3.8 a	16	1.76 ± 0.24

762 **Table 3.** Influences of calendar year, cambial age and tree diameter (dbh) on basal area increment (BAI) of silver fir at the three study sites and
763 considering two dieback classes according to the best-fit generalized additive mixed models. For each site and tree type, the number of measured
764 tree-rings is shown. The influence of the covariates affecting BAI is indicated by the *F* statistic and its associated probability (*P*). In addition, the
765 estimated degrees of freedom (*edf*) for each variable are shown. The amount of variance explained by each model (R^2) is indicated in the last
766 column.
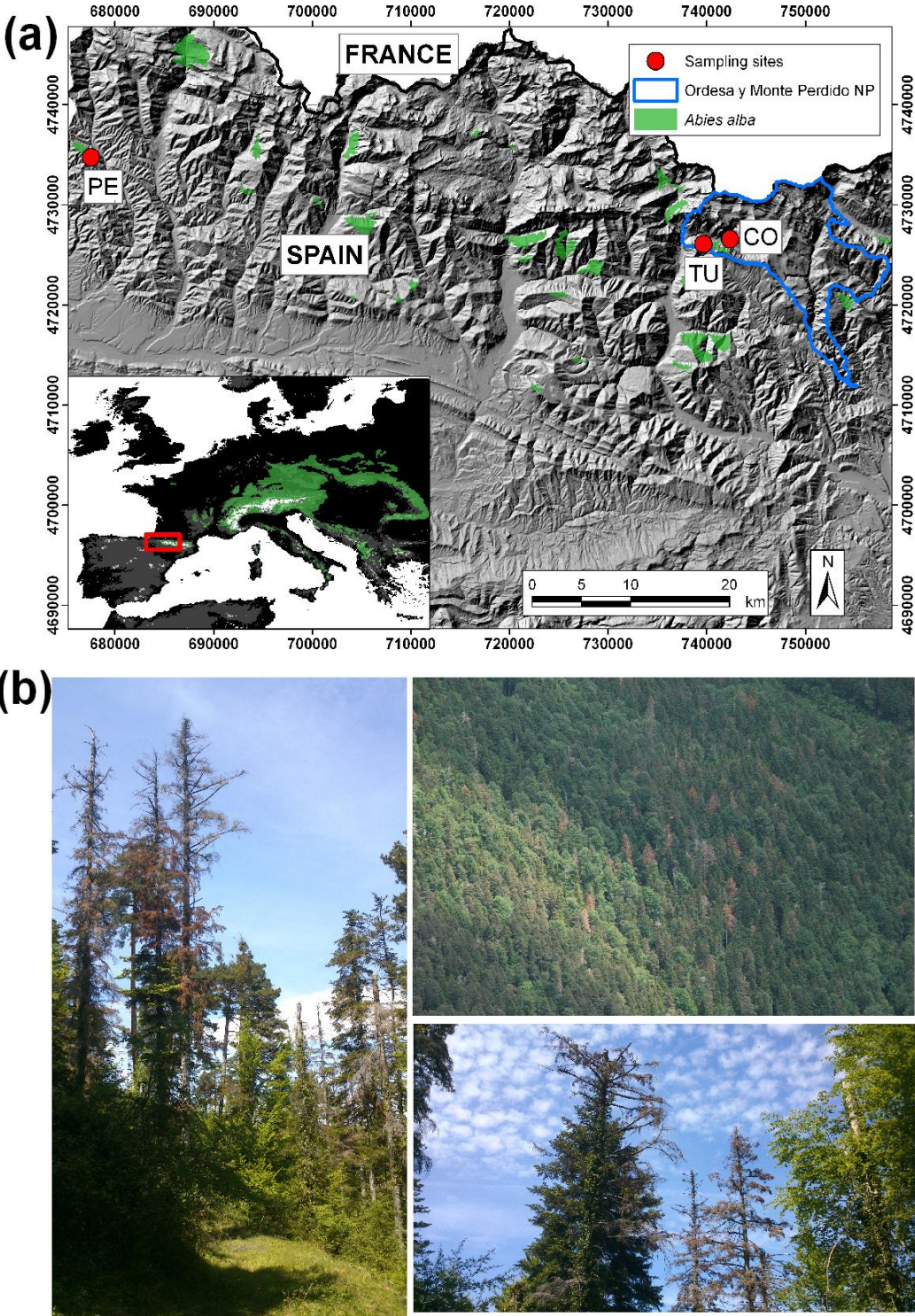
767

Site	Tree type	No. tree rings	Year			Age			Dbh			R^2
			edf	*F*	*P*	*edf*	*F*	*P*	*edf*	*F*	*P*	
Cotatuero	Non-declining	2672	2.68	4.09	0.009	1.00	23.10	<0.001	2.39	142.01	<0.001	0.69
	Declining	3092	4.02	14.77	<0.001	1.60	2.01	0.139	3.38	21.39	<0.001	0.43
Turieto	Non-declining	1985	6.97	8.56	<0.001	1.00	2.23	0.135	1.00	99.76	<0.001	0.60
	Declining	1316	4.15	12.34	<0.001	1.00	4.65	0.031	1.00	44.36	<0.001	0.54
Paco Ezpela	Non-declining	1703	7.21	15.15	<0.001	1.00	1.16	0.281	2.91	18.48	<0.001	0.53
	Declining	2128	6.51	18.85	<0.001	1.00	2.10	0.148	1.00	46.78	<0.001	0.45

768

769

770 **Table 4.** Best linear mixed-effects models of basal-area increment (BAI) of silver fir

771 fitted to trees from the three study sites (Cotatuero, Turieto and Paco Ezpela) as a

772 function of climatic variables and the competition index (CI). A null model considering

773 BAI as a constant was also included. Tree age and the tree code were used as random

774 effects. Abbreviations: CI, competition index; *n*, number of trees analysed; PFA,

775 previous autumn precipitation; PWI, previous-winter precipitation; SPEI, August 4-

776 month SPEI values; TMSp, spring mean maximum temperature; TmWI, previous

777 winter mean minimum temperature; DF, degrees freedom; *Wi*, relative probability that

778 model *i* is the best model for the observed data.

779

780

Site	Tree type	*n* trees	DF	Selected model	*Wi*
Cotatuero	Non declining	17	992	0.19 SPEI − 0.01 PWI − 0.04 CI	0.49
	Declining	15	861	0.42 SPEI − 0.01 PWI −0.17 TmWI − 0.12 CI	0.34
Turieto	Non declining	16	924	0.48 SPEI − 0.19 TmWI − 0.23 CI	0.78
	Declining	8	466	0.73 SPEI − 0.17 TmWI− 0.16 CI	0.45
Paco Ezpela	Non declining	10	646	1.65 SPEI + 0.66 TMSp − 0.07 CI	0.86
	Declining	16	941	1.59 SPEI + 0.01 PFA − 0.44 CI	0.99

781

782 **Table 5.** Isolation frequency of different fungi inhabiting stem and root wood of silver

783 fir trees at three study sites in the Pyrenees. Observed and expected (in parentheses)

784 frequencies are shown separately depending on the symptoms for declining (including

785 recently dead trees) and non-declining trees. The probability (P) values associated with

786 the χ^2 statistic were calculated for each fungus found in at least two trees.

787

Fungi species	Declining trees	Non-declining trees	χ^2 (P)
Amylostereum chailletii (Pers.) Boidin	8 (4)	0 (4)	6.125 (0.013)
Armillaria spp. (Fr.) Staude	1	0	–
Hericium erinaceus (Bull.) Pers.	1	0	–
Heterobasidion annosum (Fr.) Bref.	5 (3)	1 (3)	1.500 (0.221)
Hypholoma acutum (Sacc.) E. Horak	0	1	–
Hypocrea lixii Pat.	1	0	–
Ganoderma lucidum (Curtis) P. Karst.	1	1	–
Pholiota squarrosa (Vahl) P. Kumm.	1	1	–
Porodaedalea pini (Brot.) Murrill	1	0	–
Trichaptum abietinum (Dicks.) Ryvarden	4 (3)	2 (3)	0.167 (0.683)
Volutella ciliata (Alb. And Schwein.) Fr.	0	2	–

788

789

Figures

Figure 1

793

794   **Figure 2**

795

796   **Figure 3**